

12

REPORT NO. NADC-82007-60

AD-A132691



AN ANALYSIS OF THE FLOW TURNING CHARACTERISTICS OF UPPER-SURFACE BLOWING DEVICES FOR STOL AIRCRAFT

Dr K.T. Yen
King of Prussia Center
THE PENNSYLVANIA STATE UNIVERSITY
650 S. Henderson Road
King of Prussia, PA 19406

OCTOBER 1982

FINAL REPORT
AIRTASK NO. A03V-320D/001B/7F41-400-00
Contract No. N62269-82-M-3070

Approved for Public Release; Distribution Unlimited

DTIC
SELECTE
SEP 20 1983
S E D

Prepared for
Aircraft and Crew Systems Technology Directorate (Code 6053)
NAVAL AIR DEVELOPMENT CENTER
Warminster, PA 18974

DTIC FILE COPY

88 00 19 01

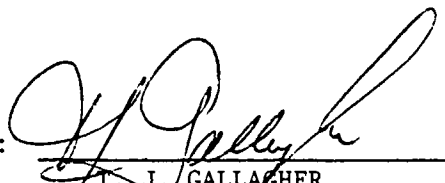
N O T I C E S

REPORT NUMBERING SYSTEM - The numbering of technical project reports issued by the Naval Air Development Center is arranged for specific identification purposes. Each number consists of the Center acronym, the calendar year in which the number was assigned, the sequence number of the report within the specific calendar year, and the official 2-digit correspondence code of the Command Office or the Functional Directorate responsible for the report. For example: Report No. NADC-78015-20 indicates the fifteenth Center report for the year 1978, and prepared by the Systems Directorate. The numerical codes are as follows:

CODE	OFFICE OR DIRECTORATE
00	Commander, Naval Air Development Center
01	Technical Director, Naval Air Development Center
02	Comptroller
10	Directorate Command Projects
20	Systems Directorate
30	Sensors & Avionics Technology Directorate
40	Communication & Navigation Technology Directorate
50	Software Computer Directorate
60	Aircraft & Crew Systems Technology Directorate
70	Planning Assessment Resources
80	Engineering Support Group

PRODUCT ENDORSEMENT - The discussion or instructions concerning commercial products herein do not constitute an endorsement by the Government nor do they convey or imply the license or right to use such products.

APPROVED BY:



T. J. GALLAGHER
CAPT, MSC, USN

DATE:



1 September 1983

UNCLASSIFIED

SECURITY CLASSIFICATION OF THIS PAGE (When Data Entered)

REPORT DOCUMENTATION PAGE		READ INSTRUCTIONS BEFORE COMPLETING FORM
1 REPORT NUMBER NADC-82007-60	2. GOVT ACCESSION NO. AD - A132691	3 RECIPIENT'S CATALOG NUMBER
4 TITLE (and Subtitle) An Analysis of the Flow Turning Characteristics of Upper Surface Blowing Devices for STOL Aircraft		5 TYPE OF REPORT & PERIOD COVERED Final ; July-October 1982
		6 PERFORMING ORG. REPORT NUMBER
7 AUTHOR(s) K. T. Yen	8. CONTRACT OR GRANT NUMBER(s) N62269-82-M-3070	
9 PERFORMING ORGANIZATION NAME AND ADDRESS King of Prussia Center, Pennsylvania State U. 650 S. Henderson Road King of Prussia, PA 19406		10 PROGRAM ELEMENT, PROJECT, TASK AREA & WORK UNIT NUMBERS Airtask No. A03V-320D/001B/7F41-400-000
11. CONTROLLING OFFICE NAME AND ADDRESS Aircraft and Crew Systems Technology Directorate (Code 6053) NAVAL AIR DEVELOPMENT CENTER Warminster, PA 18974		12. REPORT DATE October 1982
		13 NUMBER OF PAGES 40
14 MONITORING AGENCY NAME & ADDRESS (if different from Controlling Office)		15 SECURITY CLASS. (of this report) Unclassified
		15a DECLASSIFICATION/DOWNGRADING SCHEDULE
16 DISTRIBUTION STATEMENT (of this Report) Approved for Public Release; Distribution Unlimited		
17 DISTRIBUTION STATEMENT (of the abstract entered in Block 20, if different from Report)		
18 SUPPLEMENTARY NOTES		
19 KEY WORDS (Continue on reverse side if necessary and identify by block number) STOL Upper-surface blown flaps Flow turning		
20 ABSTRACT (Continue on reverse side if necessary and identify by block number) Experimental data from wind-tunnel tests on the static flow turning performance of upper-surface blown (USB) flaps have been assembled, analyzed, and correlated in the present study. Formulas for calculating the flow turning angle and flow turning efficiency have been derived for rectangular nozzles with radius flaps. In the formula for the flow turning angle, the variables are the flap angle, the aspect ratio of the nozzle, the ratio of the flap radius to the nozzle height, and the roof and spread angles of the nozzle.		

DD FORM 1 JAN 73 1473

EDITION OF 1 NOV 65 IS OBSOLETE
S/N 0102-LF-014-6601

UNCLASSIFIED

SECURITY CLASSIFICATION OF THIS PAGE (When Data Entered)

20. (Continued)

A method for calculating the flow turning angle of arbitrary USB configurations has been outlined. This method accounts by means of parameters for the different geometry of the nozzles, the differences in the flaps, and the effect of installation of USB systems on aircraft. Because of insufficient data base, these formulas have not been completely verified.

Accession For	
NTIS	<input checked="" type="checkbox"/>
DAIR	<input type="checkbox"/>
Unpublished	<input type="checkbox"/>
Justification	
By _____	
Distribution/ _____	
Availability Codes	
Dist	Special
A	

1975
 10/10/75
 10/10/75

UNCLASSIFIED

TABLE OF CONTENTS

	Page
TABLE OF CONTENTS.....	ii
LIST OF FIGURES.....	iii
LIST OF SYMBOLS.....	iv
LIST OF TABLES.....	iv
PREFACE.....	1
SUMMARY.....	2
INTRODUCTION.....	3
I. FLOW TURNING CHARACTERISTICS OF UPPER-SURFACE BLOWN FLAPS.....	5
II. ANALYSIS OF EXPERIMENTAL DATA ON THE FLOW TURNING	
CHARACTERISTICS OF USB FLAPS.....	7
1. The Basic Configuration of Rectangular Nozzles	
and Radius Flaps.....	7
2. Other Configurations of USB Flap Systems.....	8
a. Rectangular Nozzles with a Radius Flap	
Installed on an Aircraft Model.....	9
b. Rectangular Nozzles with a Double-Slotted	
Flap Installed on an Aircraft Model.....	10
c. D-Nozzles with a Double-Slotted Flap	
Installed on an Aircraft Model.....	10
III. DEVELOPMENT OF PREDICTION METHODS FOR THE TURNING	
CHARACTERISTICS OF USB FLAPS.....	12
1. The Basic Configuration of Rectangular Nozzles	
and Radius Flaps.....	12
2. Other Configurations of USB Flap Systems.....	14
a. Determination of K_G	15
b. Determination of K_F	16
c. Determination of K_I	16
IV. SOME REMARKS ON THE AERODYNAMICS OF USB FLAP SYSTEMS.....	18
V. CONCLUDING REMARKS AND RECOMMENDATIONS.....	20
REFERENCES.....	21

LIST OF FIGURES

Figure		Page
1	Upper-Surface Blown Flap.....	23
2	Summary of Static Turning Characteristics.....	24
3	Model Configuration Used in Static Test of USB Nozzle and Flap Variables (Reference 3).....	25
4	Effect of Pressure Ratio on Flow Turning for Various Nozzle Aspect Ratios.....	25
5	Effect of Pressure Ratio on Flow Turning for a Range of Flap Radius. Nozzle Aspect Ratio of 28.....	26
6	Effect of Flap Radius of Flow Turning for a Pressure Ratio of 1.4 and a Constant Run Length.....	26
7	Effects of Nozzle Roof Angle and Spread Angle on Flow Turning.....	27
8	Details of Nacelles and Aspect-Ratio-6 Rectangular Nozzles.....	28
9	Radius Flap High-Lift System.....	29
10	Variation of Static Turning Angle and Turning Efficiency with Static Thrust. Rectangular Nozzles and Radius Flap.....	30
11	Variation of Static Turning Angle and Turning Efficiency with Twin-Engine Simulation. Rectangular Nozzles and Radius Flap.....	31
12	Basic High Lift System with Double-Slotted Flap.....	32
13	Variation of Static Turning Angle and Turning Efficiency. Rectangular Nozzles and Basic Flap.....	33
14	Variation of Static Turning Angle and Turning Efficiency with Twin-Engine Simulation. Rectangular Nozzles and Basic Flap.....	34
15	Details of Nacelles and D-Nozzles.....	35
16	Variation of Static Turning Angle and Turning Efficiency with Static Thrust. D-Nozzles and Basic Flap.....	36
17	Static Turning Angle for Rectangular Nozzles with Aspect Ratio Equal to 6 and Various Flap Systems.....	37
18	Static Turning Angle for Rectangular Nozzles and Various Flap.... Systems	38

LIST OF SYMBOLS

Only dimensionless quantities are dealt with in the study. Consequently, all units for dimensional quantities are omitted.

A	Area of nozzle
AR	Aspect ratio of nozzle
ΔC_{ℓ}	Incremental lift coefficient
b_r	Power for nozzle roof angle
b_s	Power for nozzle spread angle
c_r	Coefficient for nozzle roof angle
c_s	Coefficeint for nozzle spread angle
C_u	Thrust coefficient
F_A	Axial force
F_N	Normal force
h	Nozzle height
K	Parameter (equation (6))
K_G, K_F, K_I	Parameters (equation (9))
r	Flap radius
w	Nozzle width
δ_F	Flap angle (figure 1)
$\delta_{F\ell}$	Flap angle at the lower surface (figure 1)
δ_j	Flow turning angle
$\delta_{j,max}$	Maximum flow turning angle (equation (9))
$\delta_{j,a}$	Flow turning angle of arbitrary configuration
$\delta_{j,b}$	Flow turning angle of basic configuration
δ_r	Roof angle of nozzle
δ_s	Spread angle of nozzle
δ_s^*	Deflection angle of leading-edge slat (figure 16)
η	Flow turning efficiency
λ	Power in (r/h) for flow turning angle

LIST OF TABLES

Table		Page
1	Experimental Data.....	39

PREFACE

The research reported herein was performed by the King of Prussia Center, Graduate Studies and Continuing Education, The Pennsylvania State University, during the period from July 1 to October 22, 1982. With Dr. K. T. Yen as the Principal Investigator, the sponsorship was provided by the Naval Air Development Center, Warminster, PA, under the Contract No. N62269-82-M-3070. The NADC technical monitor was Mr. Campbell Henderson, whose technical support and many helpful suggestions are acknowledged.

SUMMARY

Experimental data from wind-tunnel tests on the static flow turning performance of upper-surface blown (USB) flaps have been assembled, analyzed, and correlated in the present study. Formulas for calculating the flow turning angle and flow turning efficiency have been derived for rectangular nozzles with radius flaps. In the formula for the flow turning angle, the variables are the flap angle, the aspect ratio of the nozzle, the ratio of the flap radius to the nozzle height, and the roof and spread angles of the nozzle. A method for calculating the flow turning angle of arbitrary USB configurations has been outlined. This method accounts by means of parameters for the different geometry of the nozzles, the differences in the flaps, and the effect of installation of USB systems on aircraft. Because of an insufficient data base these formulas have not been completely verified.

INTRODUCTION

The basic concept and application of powered lift and the effects of some fundamental design variables have been reviewed and discussed by Campbell in 1976 (reference 1). The two "externally blown systems" of the powered lift, i.e., the externally blown flap and the upper-surface blown flap have the advantage that no internal ducting is needed, although the internally blown flaps are more efficient.

The upper-surface blown (USB) flap concept has been found to be generally quieter than the other concepts because the wing tended to act as a noise shield producing more noise above the wing but much less noise below the wing.

Research on both the aerodynamic and noise characteristics of the USB concept was first conducted at the NASA/Langley Research Center during the latter part of the 1950's. Serious interest and research in the concept was resumed in the early 1970's, and carried out at an accelerated pace in the development of the USAF YC-14 Advanced Medium STOL Transport. The USB concept has been successfully demonstrated in the flight of YC-14 in 1976 as well as the NASA quiet short-haul research aircraft (QSRA).

In 1980, a V/STOL Aerodynamics and Stability & Control Manual was published by the Flight Dynamics Branch of the Naval Air Development Center (reference 2). With Navy's interest in the development of future STOL aircraft, the sections of the Manual relating to STOL aircraft concepts and prediction methods are being developed in preparation for issuance of the STOL aircraft supplement of the Manual. In the development of engineering prediction methods for USB configurations, it is recognized that a primary aerodynamic/propulsive characteristic relates to the turning performance of the system. Predictions of static turning performance offer a means of evaluating the high lift potential of these configurations as well as providing the basepoint parametric values of momentum flux needed to correlate and predict the aerodynamic characteristics of STOL aircraft.

A review of literature on USB flaps revealed that no known prediction methods for the turning performance is available at the present time. A cursory examination of the aerodynamic characteristics of USB systems shows that the problem is highly complex and is not easily amenable to analytical treatment or solved by computational aerodynamic techniques. It is considered likely that

for the foreseeable future any prediction method development must be based on experimental data, and will lead to largely empirical methods.

Although a large amount of data on the static turning performance of USB systems exists (references 3-11), it appears that a systematic analysis of the data has not yet been done. The purpose of the present study is first to assemble, analyze, and correlate the available data. Secondly, from these results, empirical or semi-empirical methods for the prediction of flow turning performance of arbitrary USB configurations are developed, and the range of their applicability determined.

It is noted that in order to develop prediction methods for arbitrary USB configurations an adequate data base for arbitrary USB configurations is necessary. In evaluating available data, only the work by Sleeman and Phelps (reference 3) was found to have reported turning performance data for a large number of geometric and flow variables. Consequently, requests were made to Arthur E. Phelps III as well as Joseph L. Johnson, Jr. of NASA/Langley Research Center for experimental data in addition to those reported in reference 3. Unfortunately, due to the termination of V/STOL work at NASA/Langley Research Center, the data were scattered and are no longer available (reference 12). In view of the inadequate data base, the prediction methods developed can only be considered as preliminary because the parameters and coefficients cannot be accurately determined at the present time.

The report summarizes results from the present study of turning performance of USB flap systems. Formulas for calculating the turning performance have been derived for rectangular nozzles with radius flaps based on correlating the available data (reference 3). A method for calculating the turning performance of other types of nozzles and flaps is outlined using the rectangular nozzles and radius flaps as the basic case.

I. FLOW TURNING CHARACTERISTICS OF UPPER-SURFACE BLOWN FLAPS

A typical USB nozzle and flap system is shown in the lower sketch of figure 1. The turning of the engine efflux is effected and controlled by the deflection of the flap. The flow turning angle is defined by

$$\delta_j = \tan^{-1} \sqrt{\frac{F_N}{-F_A}} \quad (1)$$

where F_N and F_A are the axial and normal forces acting on the USB system and are measured experimentally. The turning efficiency η is defined by

$$\eta = \frac{\sqrt{F_N^2 + F_A^2}}{T} \quad (2)$$

where T is the thrust of the engine efflux.

The flap angle δ_f used in the present study is the deflection angle of the upper surface at the trailing edge of the flap (figure 1). In many experimental studies (e.g., reference 6), the flap angle is considered as the angle of the lower surface of the flap, i.e., $\delta_{f\ell}$ in figure 1. However, it is considered more meaningful for the present analysis to use δ_f as the flap angle.

In addition to δ_j and δ_f , there are other geometric variables for the nozzle-flap system as shown in figure 1, i.e.,

Flap radius r

Nozzle width w and height h

Nozzle roof angle δ_r and spread angle δ_s

Evidently, the shape of the upper surface of the flap will play a significant role in the flow turning. Some important flow parameters for USB flap systems are the pressure ratio of the engine efflux and the boundary layer flow conditions over the flap.

Some typical experimental results for the static turning angle δ_j are shown in figure 2. These results are taken from the wind-tunnel investigation by Smith, Phelps and Copeland (reference 4) for a large-scale

semispan model with an unswept wing and an upper-surface blown flap. Figure 2 shows that at a lower flap setting, $\delta_f = 32^\circ$, the flow turning angle δ_j is nearly the same as δ_f . At the higher flap setting, $\delta_f = 72^\circ$, the flow turning angle δ_j is substantially less (nearly by 10°). This suggests that at the higher setting, the flow cannot follow the flap surface and some flow separation has occurred. The flow turning efficiency is also higher at the lower flap setting, 95 percent at $\delta_f = 32^\circ$, and is about 85 percent at $\delta_f = 72^\circ$. In figure 2, the shaded band summarizes representative values of static turning performance obtained from a number of experimental investigations (reference 13) indicating that in general efficiencies from about 80 - 95 percent can be obtained. (Note in reference 4, a free-stream dynamic pressure of 79N/m^2 (1.65 lb/ft^2) was used for C_μ .)

For a designer of USB flap systems, it is important to arrive at an optimum configuration within the design limits for maximum flow turning efficiencies. At the present time, a designer must rely on his experience and extensive wind-tunnel investigations to achieve this goal, often without realizing an optimum design. It is evidently desirable to have an analytical tool as an aid in the design process. Empirical formulas, with obvious limited validity, can offer some help, and it is the purpose of the present study to derive some empirical formulas for the prediction of the static turning performance of USB systems.

II. ANALYSIS OF EXPERIMENTAL DATA ON THE FLOW TURNING CHARACTERISTICS OF USB FLAPS

Considerable efforts were expended in assembling all available data on the flow turning performance of USB flaps (reference 14). Table 1 summarizes the available experimental data. It is noted that the data sources are NASA/Langley Research Center publications. As mentioned in the Introduction, additional data were obtained in the experiments conducted at NASA/Langley Research Center and not reported in the publications. Unfortunately, the additional data were no longer available (reference 12).

In evaluating the available data, the work by Sleeman and Phelps (reference 3) for rectangular nozzles and radius flaps is found to be the only one with a systematic variation of the geometric variables for both the nozzle and flap, although for only one flap angle $\delta_f = 90^\circ$. In the work by Smith, Phelps and Copeland (reference 4), the only variation in the rectangular nozzle is in the aspect ratio (2, 4 and 6), and the three flap angles are $\delta_f = 72^\circ$, 52° and 32° . In other works, listed in Table 1, generally one nozzle configuration and one flap system were tested. Consequently, the work by Sleeman and Phelps for rectangular nozzles and radius flaps is adopted in the present study as the basic case for the data analysis as well as for the development of a prediction method to be presented in the next section.

1. The Basic Configuration of Rectangular Nozzles and Radius Flaps

A schematic drawing of the model used in Sleeman and Phelps' experiments is given in figure 3 to indicate configuration variables investigated. Eight values of nozzle height were investigated by the use of interchangeable nozzle blocks; seven values of flap radius were investigated with circular arc flaps; five values of run length ahead of the flap were investigated, but values of run length were not given in the data reported in reference 3. The flap angle was set at 90° .

Data showing effects of nozzle pressure ratio on flow turning for

various nozzle pressure ratios are presented in figure 4. The results show turning angles up to 50° indicating that the jet flow did not adhere to the 90° flap all along the flap but separated at some point ahead of the trailing edge. As the jet height increased with decreased nozzle aspect ratio, there occurred at higher pressure ratios abrupt loss in flow turning suggesting sudden detachment of the flow. In general, such sudden detachment can occur if the flap radius is too small, the jet is too thick, or the pressure ratio is too high.

Effects of pressure ratio on flow turning for a range of flap radius over nozzle height are shown in figure 5. It is of interest to note that the flow turning is fairly insensitive to pressure ratio, except a sudden drop did occur for the ratio of flap radius to nozzle height equal to 4 at the pressure ratio of about 2.2.

Test results show that low pressure ratios (<1.5) were found to be indicative of the maximum flow turning to be expected from a given configuration. Figure 6 shows effects of flap radius on flow turning over a broad range of nozzle aspect ratios for a pressure ratio of 1.4. At low values of flap radius/height ratio, a breakaway point in flow turning is evident.

Effect of systematic variations in roof angle δ_r and spread angle δ_s are shown in figure 7 for the ratio of flap radius to nozzle height equal to 4 and nozzle aspect ratio of 7. Substantial increases in flow turning can be achieved by an increase in δ_r or δ_s or a combination of δ_r and δ_s . Although the effect of nozzle roof angle is to thin the middle part of the jet while that of spread angle is to thin the edges of the jet, the trade-offs in roof and spread angles can provide the designer with some freedom in selection to minimize problems such as high cruise drag associated with high boattail-roof angles.

2. Other Configurations of USB Flap Systems

In the present study, a unit of a nozzle and a flap such as the basic configuration will be designated as a "not installed" USB system. When such a unit is put on an aircraft, the USB system is called installed.

In the following, the static turning performances of other USB flap systems will be reviewed and compared with that of the basic configuration.

a. Rectangular Nozzles with a Radius Flap Installed on an Aircraft Model

In reference 6, an investigation was conducted in the Langley V/STOL tunnel to determine the aerodynamic performance of a four-engine USB transport configuration. The supercritical wing has an aspect ratio of 7.48. Tests were conducted with D-nozzles and rectangular nozzles with an aspect ratio of 6.0, and both a double-slotted airfoil flap and a radius flap.

Details of the rectangular nozzles are shown in figure 8. The aft parts of the nozzles are not symmetrical, but with opposite flare for the inboard and outboard nacelles. The highlift radius flap system is shown in figure 9. The radius of the flap is equal to 0.3 chord (local). The angle δ_{fl} in figure 10 refers to the lower surface of the flap (figure 1), and the flap angle δ_f is estimated to be approximately 12° larger than δ_{fl} .

The data for the static turning performance of the rectangular nozzles with the radius flap are shown in figure 10. An important characteristic in the static turning is the small variation in δ_j with increasing thrust (compared with that of D-nozzles) for all flap deflections. Sleeman and Hohlweg in reference 6 suggested that the reason is that the jet flow was fairly well stabilized over the radius flap even though the full flow turning was not achieved. The turning effectiveness of the radius flap was about two thirds for all flap deflections investigated, i.e, asymptotically at full thrust

$$\delta_j = \frac{2}{3} \delta_f \quad (3)$$

Static tests were made with either the inboard engines or the outboard engines shut off to simulate power effects, and the results are given in figure 11. The data show that approximately 10°

greater turning was achieved with only the outboard engines operating. In addition, the static turning for all outboard engines alone was around 90 percent of the turning for all engines operating. Similar results were obtained for the turning efficiency. Thus, there was considerable interaction between the inboard and outboard engines in the flow turning performance, and the static turning for the outboard and inboard engines alone are not additive. This interaction will be further discussed in the next section.

b. Rectangular Nozzles with a Double-Slotted Flap Installed on an Aircraft Model

In reference 6, tests were also made with a double-slotted flap shown in figure 12. Deflections of the flap up to $\delta_{fl} = 50^\circ$ show smooth flow turning. But at $\delta_{fl} = 65^\circ$ the flow turning angle δ_j drops below that at $\delta_{fl} = 50^\circ$ at higher thrust, indicating progressive flow detachment. The flow turning efficiency is also correspondingly lower. The effects of two-engine power simulation for this configuration is shown in figure 14. The results are similar in characteristics to those for a radius flap (figure 11).

c. D-Nozzles with a Double-Slotted Flap Installed on an Aircraft Model

D-nozzles of the form shown in figure 15 with a double-slotted flap were tested in the Langley V/STOL tunnel (reference 6). Figure 16 shows that the turning performance is substantially lower than that with the rectangular nozzles with either the radius flap or the double-slotted flap. Note that the D-nozzles have a 14° roof angle but zero spread angle.

The results for turning angle for rectangular nozzles with aspect ratio equal to 6 from the experiments listed in Table 1 are summarized in figure 17. The only calculated result is that for a radius flap with $\delta_r = 23^\circ$, $\delta_s = 15^\circ$ and $r/h = 3.2$. The value of $\delta_j = 70.6$ for $\delta_f = 90^\circ$ is estimated based on Sleeman and Phelps' data of reference 3. The straight line passing through the calculated point has the slope of 2/3 indicating an estimate of the variation of δ_j with δ_f in the manner of equation (3).

An examination of figure 17 shows that:

- (i) rectangular nozzles with radius flaps when installed on an aircraft model yield smaller values of δ_j than those not installed;
- (ii) rectangular nozzles with an airfoil flap have generally higher values of δ_j than the rectangular nozzles with a radius flap.

Similar results can be seen from figure 18, in which δ_j/δ_f is plotted versus the nozzle aspect ratio. The calculated results for the same nozzles given in figure 17 are again estimates based on Sleeman and Phelps' experimental data (reference 3). The only experimental work for aspect ratios 2, 4 and 6 is that by Smith, Phelps and Copeland (reference 4). However, the variation of δ_j/δ_f with the aspect ratio from the experimental work is very different from that calculated for reasons not yet understood. The flow turning angles for D nozzles given in reference 8 are also plotted in figure 18.

In concluding the data analysis, it can be stated that:

- (i) the nozzles used in the different experiments listed in Table 1 are generally not of the same configuration,
- (ii) the flap systems used are generally not the same,
- (iii) the nozzle-flap systems are generally not installed on aircraft with the same configurations.

Evidently, the different experiments are directed at specific USB systems to provide needed information concerning the turning performance and other aerodynamic characteristics. However, in order to achieve a basic understanding of the aerodynamics of USB flaps, or to develop prediction methods for the turning performance for arbitrary USB configuration more experimental data of the type obtained by Sleeman and Phelps (reference 3) are needed to provide an adequate base.

III. DEVELOPMENT OF PREDICTION METHODS FOR THE TURNING CHARACTERISTICS OF USB FLAPS

The development of prediction methods consists of two parts, i.e., that for the basic configuration of rectangular nozzles and radius flaps, and that for arbitrary USB configuration. The experimental data obtained by Sleeman and Phelps (reference 3) are used to derive an empirical formula for the flow turning angle δ_j . Another empirical formula is then used to calculate the flow turning efficiency η with δ_j known.

For USB flap systems with arbitrary configurations, a formula for the flow turning is obtained by introducing into the formula for the basic configuration parameters to account for the nozzle geometry, flap characteristics, and other features.

1. The Basic Configuration of Rectangular Nozzles and Radius Flaps

By using Sleeman and Phelps' data given in figures 5 and 6 showing the dependence of δ_j on the ratio of flap radius to nozzle height for a range of pressure ratios, a formula for δ_j can be found. First, it is assumed that $\delta_j \sim (r/h)^\lambda$, and λ is insensitive to variations in the pressure ratio. Using the results for the pressure ratio at 1.4 it is found that for $AR = 28$

$$\delta_j \sim \left(\frac{r}{h}\right)^{-.104} \quad (4)$$

The value of $\lambda = -.104$ corresponds to a coefficient of determination of .94.

However, from figure 6, δ is found to vary slightly with AR . For example, at $AR = 28, 14$ and 3.5 , the values of λ are estimated to be $-.104, -.099$ and $-.091$, respectively. The variation can be approximated by

$$\lambda = -.084AR^{.06}$$

The results of figure 6 for the lower values of radius range shows the existence of a breakaway point beyond which little or no flow turning is available. In addition, as the flap radius is reduced at a fixed aspect ratio of low value (below or equal to 9.3), the flow turning angle will decrease before the break-

away point is reached. This characteristic cannot be calculated by using a formula of the type shown in equation (4).

It is of interest to note that Henderson (reference 15) obtained from data correlation a formula for the incremental lift due to blowing for a two-dimensional circulation-control airfoil as follows

$$\Delta C_L \sim \left(\frac{r}{h}\right)^{-\frac{1}{3}} \quad (5)$$

The large difference between the two powers $-\frac{1}{3}$ and $-.104$ suggests that the flow turning in the USB flap systems is not primarily a boundary layer control phenomenon as in the case of a circulation-control airfoil.

In a similar manner, the variation of δ_j with the nozzle aspect ratio can be determined from figure 4 (for a pressure ratio of 1.4) and is found to be

$$\delta_j \sim (AR)^{.5084} \quad (6)$$

It is noted that the results of figure 4 are for a constant flap radius (flap radius/nozzle height equal to 12). Since no other data is available, it is assumed that the formula will apply in general to other values of flap radius.

To account for the roof angle δ_r and spread angle δ_s , it is assumed that

$$\delta_j \sim (1 + c_r \delta_r^{b_r}) (1 + c_s \delta_s^{b_s}) \quad (7)$$

where c_r , c_s , b_r , and b_s are coefficients to be determined from the experimental data. Since only limited data are available at the present time (figure 7), these coefficients cannot yet be accurately determined. Two examples are given. For $\delta_s = 0$, it is found that $c_r = .07$ and $b_r = .82$. For small values of δ_r and δ_s (below 15°), it is found that both c_r and c_s can be approximated by $.04$ and $b_r = b_s = 1.07$ with a coefficient of determination about $.98$.

By combining the above formulas, the formula for δ_j can be written as

$$\delta_j = K \delta_f \left(\frac{r}{h}\right)^{-0.084AR^{.06}} (AR)^{.5084} (1 + c_r \delta_r^{b_r}) (1 + c_s \delta_s^{b_s}) \quad (8)$$

where K is a constant, and both δ_r and δ_s are in degrees. Based on Sleeman and Phelps' data, the value of K is approximately 0.13 for $\delta_f = 90^\circ$. However, Sleeman and Phelps have found that the value δ_j cannot increase indefinitely as (r/h) is reduced. Based on Sleeman and Phelps' data as shown in figure 6, the maximum flow turning angle is approximately (for $\delta_r = \delta_s = 0$)

$$\delta_{j, \max} = 6.69 \left(\frac{r}{h}\right)^{1.54} \quad (9)$$

Consequently, the calculated δ_j from equation (8) should be limited to $\delta_j \leq \delta_{j, \max}$. In addition, equation (8) should be used for pressure ratios below 1.75 or values at which sudden drop in δ_j occurs. With δ_j given by (8) an estimate of the flow turning efficiency η can be calculated from an empirical formula as follows

$$\eta = e^{-.0022\delta_j} \quad (10)$$

which is found to fall within the shaded band for η in figure 2.

It is noted that in deriving equation (8), the powers of r/h and AR are assumed to be independent of the pressure ratio. Although Sleeman and Phelps' data do show that δ_j is insensitive to the pressure ratio at pressure ratios below 1.75, a better approximation is to take the powers to be linearly dependent on the pressures ratio, a step not considered warranted at this time. Consequently, equation (8) does not always reproduce precisely the experimental data.

2. Other Configurations of USB Flap Systems

Using the basic configuration of rectangular nozzles and radius flaps as the

basic case, the flow turning angle for other arbitrary configurations of USB flap systems can be expressed as follows

$$\delta_{j,a} = K_G K_F K_I \delta_{j,b} \quad (11)$$

where $\delta_{j,b}$ denotes the flow turning angle for the basic case and $\delta_{j,a}$ that for an arbitrary configuration. K_G accounts for the difference in geometry of the nozzle, K_F that in the flap systems (including the effect of vortex generators), while K_I represents the modification due to installation on an aircraft. In the following, simple examples for determining the three parameters K_G , K_F , and K_I will be given.

a. Determination of K_G - Consider D-nozzles with a double-slotted flap as the arbitrary configuration installed on an aircraft (four-engine) model shown in reference 6. From figure 13 for rectangular nozzles with the same double-slotted flap at $\delta_{f\lambda} = 50^\circ$, the value of δ_j is estimated to be 49° . Thus in equation (11), the quantity $K_I \cdot \delta_{j,b}$ is equal to 49° . Next from figure 16, for D-nozzles with the same flap, the value of δ_j , i.e., $\delta_{j,a}$, at $\delta_{f\lambda} = 50^\circ$ is 28° . Consequently, with $K_F = 1$, the value of K_G is

$$K_G = \frac{28}{49} = 0.572 \quad (12)$$

If, instead of $\delta_{f\lambda} = 50^\circ$, a value of $\delta_{f\lambda} = 35^\circ$ is used, then from figures 13 and 16 the values of $\delta_{j,b}$ and $\delta_{j,a}$ are 37° and 30° , respectively. Thus, a higher value of $K_G = 30/37 = .811$ is obtained.

It would be more desirable in the method development to consider K_G as the modification factor for the difference in nozzle geometry in terms of the nozzle aspect ratio. Thus $\delta_{j,b}$ will be the flow turning angle for rectangular nozzles with an aspect ratio of w^2/A where w is the width and A the area of the arbitrary nozzle under consideration. However, there are not sufficient data available for the development of such a method.

b. Determination of K_F - Consider rectangular nozzles with a double-slotted flap as the arbitrary configuration installed on the same aircraft model shown in reference 6. The same nozzles with a radius flap will be considered as the basic configuration. From figure 10 for the basic configuration, the value of δ_j at $\delta_{fl} = 50^\circ$ is estimated to be 33.3° , i.e., $K_I \cdot \delta_{j,b} = 33.3^\circ$. From figure 13, the value of δ_j is 49° for rectangular nozzles with the double-slotted flap, i.e., $\delta_{j,a} = 49^\circ$. Consequently, with $K_G = 1$,

$$K_F = \frac{49}{33.3} = 1.47 \quad (13)$$

c. Determination of K_I - Two cases will be considered, i.e., a single-engine installation and a twin-engine installation of USB flap systems.

Single-engine Installation - Consider rectangular nozzles with an aspect ratio equal to 6 and a radius flap. From figure 17, the value of δ_j at $\delta_f = 72^\circ$ is 49° for the rectangular nozzles installed as shown in reference 6. For rectangular nozzles with $\delta_r = 23^\circ$, $\delta_s = 15^\circ$, $r/h = 3.2$, the value of δ_j at $\delta_f = 72^\circ$ can be estimated from the straight line passing through the calculated point in figure 17 as 58° . Consequently, the value of $\delta_{j,a}$ is 49° , and that of $\delta_{j,b}$ is 58° . With $K_G = K_F = 1$, the value of K_I is

$$K_I = \frac{49}{58} = .845 \quad (14)$$

Values of K_I 's smaller than 1 may be regarded as the results of installation loss in the flow turning.

Twin-engine Installation - As mentioned in the preceding section and shown in figures 11 and 14, in a twin-engine installation, there is considerable interaction between the inboard and outboard engines. It is noted that both the turning angle and efficiency are higher when all engines are operating, but not additive.

Consider rectangular nozzles (AR = 6) with a radius flap (figure 9). From figure 17, at $\delta_{fl} = 75^\circ$ ($\delta_f = 87^\circ$) the value of δ_j is approximately 68° . From

figures 10 and 11, the values of δ_j for all engines running is 49° , while those for outboard and inboard engines running are 45° and 35° , respectively. The values of K_I 's are

$$\begin{aligned} K_I \text{ for all engines running} &= .72 \\ K_I \text{ for outboard engines running} &= .66 \\ K_I \text{ for inboard engines running} &= .51 \end{aligned}$$

The higher K_I value of .72 is evidently due to the interaction of outboard and inboard engines. The mechanism of the interaction is not yet known at the present time.

In an extreme situation, in which the two engines are close together such that the two nozzles merge into a rectangular nozzle with the aspect ratio doubled, a rough estimate of the enhanced flow turning angle may be obtained from the formula (8). Assuming that the only change is in the aspect ratio, the enhancement of δ_j will be approximately $2^{0.5084} = 1.422$. If the favorable interaction increases as the distance between the outboard and inboard engines is reduced, the value of 1.422 will be the maximum enhancement achievable. Experiments for the purpose of studying the interaction process will be needed in order to understand the mechanism and to determine accurately the values of K_I 's.

In concluding the section on the development of prediction methods, it can be stated again that a sufficient data base is clearly needed for the development of predicting methods of an empirical nature. Because of insufficient data base, the parameters and coefficients in the formulas derived in the present study can not be determined accurately. In addition, the accuracy of the formulas is difficult to assess, and some uncertainty exists in their range of applicability. Consequently, all the formulas should be regarded as preliminary at this time.

IV. SOME REMARKS ON THE AERODYNAMICS OF USB FLAP SYSTEMS

It is beyond the scope of the present study to undertake an investigation of the basic aerodynamics of USB flap systems. It is appropriate, however, to offer some remarks on the aerodynamic characteristics of the systems and the complexity and difficulty of the problem.

The action of USB flaps in providing high lift to the aircraft lies in two parts: the jet flap produced by the flow of engine exhaust offlux over the flap and the increase in wing camber due to the flap deflection.

The jet flap action is to produce a low pressure region over the flap beyond that achievable in a conventional wing with a sharp trailing edge. Pressure distributions measured over the flap surface (reference 8) show a highly complex low pressure pattern. In addition, the jet is generally quite thick such that the aerodynamic problem is three-dimensional, non-linear. The thin-jet approximation generally adopted for the analysis of jet flap is consequently not applicable.

Evidently, higher deflections of the flap are needed to produce higher curvatures for the upper surface jet flow and higher lift. However, at higher flap deflections, the flow will separate from the flap, and the USB flaps become ineffective. Moreover, in the USB systems, the sides of the jet sheet tend to roll up into vortices which in turn tend to thicken the jet, and promote a flow inboard and spanwise as well as flow separation (reference 13)

As mentioned in Section II, the flow separation often occurs as sudden detachment of the flow from the flap surface, and such sudden detachment can occur if the flap radius is too small, the pressure ratio is too high or the jet is too thick. Englar (reference 16) has summarized results of jet detachment limits for (two-dimensional) Coanda wall jets as functions of the ratio of slot height to the jet turning radius and the pressure ratio. The value of pressure ratio of 2.25, approximately, for the sudden flow detachment of the USB flap system for flap radius/nozzle height equal to 4 is shown in figure 5 and is in general accord with the experimental results given by Englar. However, figure 5 shows only one data point for sudden detachment, and no evidence of detachment at the

values of pressure ratios given and at values of flap radius/nozzle height other than 4. This characteristic does not appear to be in accord with Englar's results.

Although the separation of the flow over the flap is governed by the boundary layer characteristics of the flow, the USB flap system is not primarily a boundary-layer control device. As pointed out already, for the circulation-control airfoil, a boundary-layer control device, the lift increment is proportional to $(r/h)^{-3}$, while in the USB flap systems, the present analysis shows $\delta_j \sim (r/h)^{-10}$. Thus, in general the applicable thrust coefficient C_u for circulation-control airfoils is much smaller than 1, while the C_u values for USB flaps are of order 1. For circulation-control airfoils, the lift increment is entirely supercirculation. For USB flap systems, both supercirculation and direct lift are generally of equal significance.

It is due to the dominance of the jet action in the USB flap systems that even in wind-on conditions the free-stream Reynolds number effect will be small compared to the jet Reynolds number effect. Because of the highly turbulent nature of the engine exhaust, it is expected that the scale effect may also be small (see reference 13). It is beyond the scope of the present study to analyze the Reynolds number of the flow or the separation of boundary layers. In addition, except for the work of Smith, Phelps, and Copeland (reference 4) very little documentation of the Reynolds number of the flow is available.

In view of the complexity and difficulty of the flow problem, analytical study of the complete USB flap system does not appear to be a fruitful approach at the present time. However, many aspects of the problems can be studied analytically and such studies should be conducted. These problems will be discussed in the next section.

V. CONCLUDING REMARKS AND RECOMMENDATIONS

In the present analysis, the present data base for USB flap systems has been reviewed and found to be inadequate. This inadequacy has hampered the development of prediction methods for the turning performance of USB flap systems. It was not surprising that a literature survey did not locate any available methods.

In view of the importance of USB flap systems for STOL aircraft, it is recommended that consideration be given to additional experimental work to remedy the inadequate data base. The experimental work should be of a fundamental nature and carried out with systematic variations in the configurations of USB flaps, not directed at a specific configuration. In fact, experiments should be conducted for the purpose towards a basic understanding of the aerodynamics of USB flap systems, which ultimately will be useful to the designers to devise techniques in achieving optimum designs of USB flap systems with the desired configuration variables. The work by Sleeman and Phelps (reference 3) is the type of experimental work need to be extended by careful planning.

Since the aerodynamics of USB flaps is highly complex as remarked in the preceding section, analytical study of the complete system does not appear to be warranted at the present time. However, analysis together with appropriate experimental study is needed in several areas. It is significant to understand why USB flap systems will have reduced flow turning angles when installed on aircraft compared to the uninstalled cases. It would be also beneficial to study the flap system to determine its optimum configuration in order to delay flow separation. In the case of multi-engine aircraft, the interaction of the USB flap systems as shown in reference 6 is a significant problem which calls for additional research, both analytical and experimental. Finally, with the additional data to be made available from future experiments, it appears that the development of prediction methods initiated in the present study should be resumed. It is considered likely that for the foreseeable future such a largely empirical approach will be the most fruitful.

REFERENCES

1. Campbell, J. P., "Overview of Powered-Lift Technology." NASA SP-406, May, 1976, pp. 1-27.
2. Henderson, C., Clark, J. and Walters, M., V/STOL Aerodynamics and Stability & Control Manual, Naval Air Development Center, January, 1980.
3. Sleeman, W. C., Jr. and Phelps, A. E., III, "Upper Surface-Blowing Flow-Turning Performance." NASA SP-406, May, 1976, pp. 29-43.
4. Smith, C., Jr., Phelps, A. E., Jr. and Copeland, W. C., "Wind-Tunnel Investigation of a Large-Scale Semispan Model with an Unswept Wing and an Upper-Surface Blown Jet Flap." NASA TND-7526, February, 1974.
5. Johnson, J. L., Jr. and Phelps, A. E., III, "Low-Speed Aerodynamics of the Upper-Surface Blown Jet Flap." Society of Automotive Engineers, Paper 740470, May, 1974.
6. Sleeman, W. C., Jr. and Hohlweg, W., "Low-Speed Wind-Tunnel Investigation of a Four-Engine Upper Surface Blown Model Having a Swept Wing and Rectangular and D-Shaped Exhaust Nozzles." NASA TND-8061, December, 1975.
7. Staff of Langley Research Center, "Wind-Tunnel Investigation of Aerodynamic Performance, Steady and Vibratory Loads, Surface Temperatures, and Acoustic Characteristics of a Large-Scale Twin-Engine Upper-Surface Blown Jet-Flap Configuration." NASA TND-8235, November, 1976.
8. Hassel, J. L., Jr., "Results of Static Tests of a 1/4-scale Model of Boeing YC-14 Powered-Lift System." NASA SP-406, May, 1976, pp. 45-62.
9. Shivers, J. P., and Smith, C. C., Jr., "Preliminary Static Tests of a Simulated Upper-Surface Blown Jet-Flap Configuration Utilizing a Full-Size Turbofan Engine." NASA TND-7816, March, 1974.
10. Phelps, A. E., "Low Speed Wind-Tunnel Investigation of a Semispan STOL Jet Transport Wing-Body with an Upper-Surface Blown Jet Flap." NASA TND-7183, May, 1973.
11. Phelps, A. E., III and Smith, C. C., "Wind-Tunnel Investigation of an Upper Surface Blown Jet-Flap Powered-Lift Configuration." NASA TND-7399, December, 1973.
12. Personal communications from A. E. Phelps, III, and J. L. Johnson, Jr., July, 1982.

13. Phelps, A. E. III, Johnson, J. L., Jr., and Margason, R. J., "Summary of Low-Speed Aerodynamic Characteristics of Upper-Surface-Blown Jet-Flap Configurations." NASA 406, May, 1976, pp. 63-87.
14. A literature survey was carried out at NADC, May, 1982. Technical reports listed in Table 1 were obtained or borrowed from the Naval Air Development Center and The Pennsylvania State University. Mr. Richard E. Kuhn, formerly at NASA/Langley Research Center, and Mr. A. E. Phelps, III have kindly supplied a number of NASA reports.
15. Henderson, C., "An Engineering Method for Estimating the Aerodynamic Characteristics of Circulation Control Wings (CCW)." Naval Air Development Center, Report NADC-82186-60, June, 1982.
16. Englar, R. J., "Experimental Investigation of the High Velocity Coanda Wall Jet Applied to Bluff Trailing Edge Circulation Control Airfoils," Naval Ship Research and Development Center, TN AL-308, June, 1973.

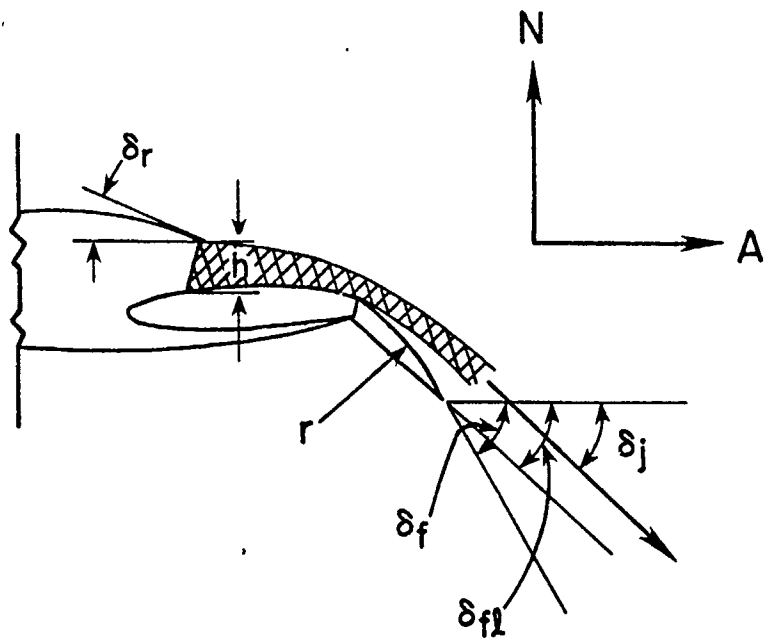
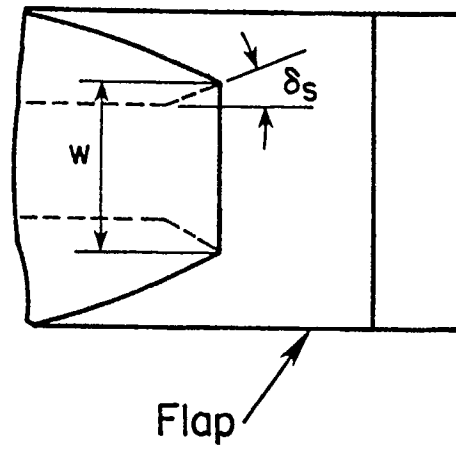


Figure 1 Upper-Surface Blown Flap

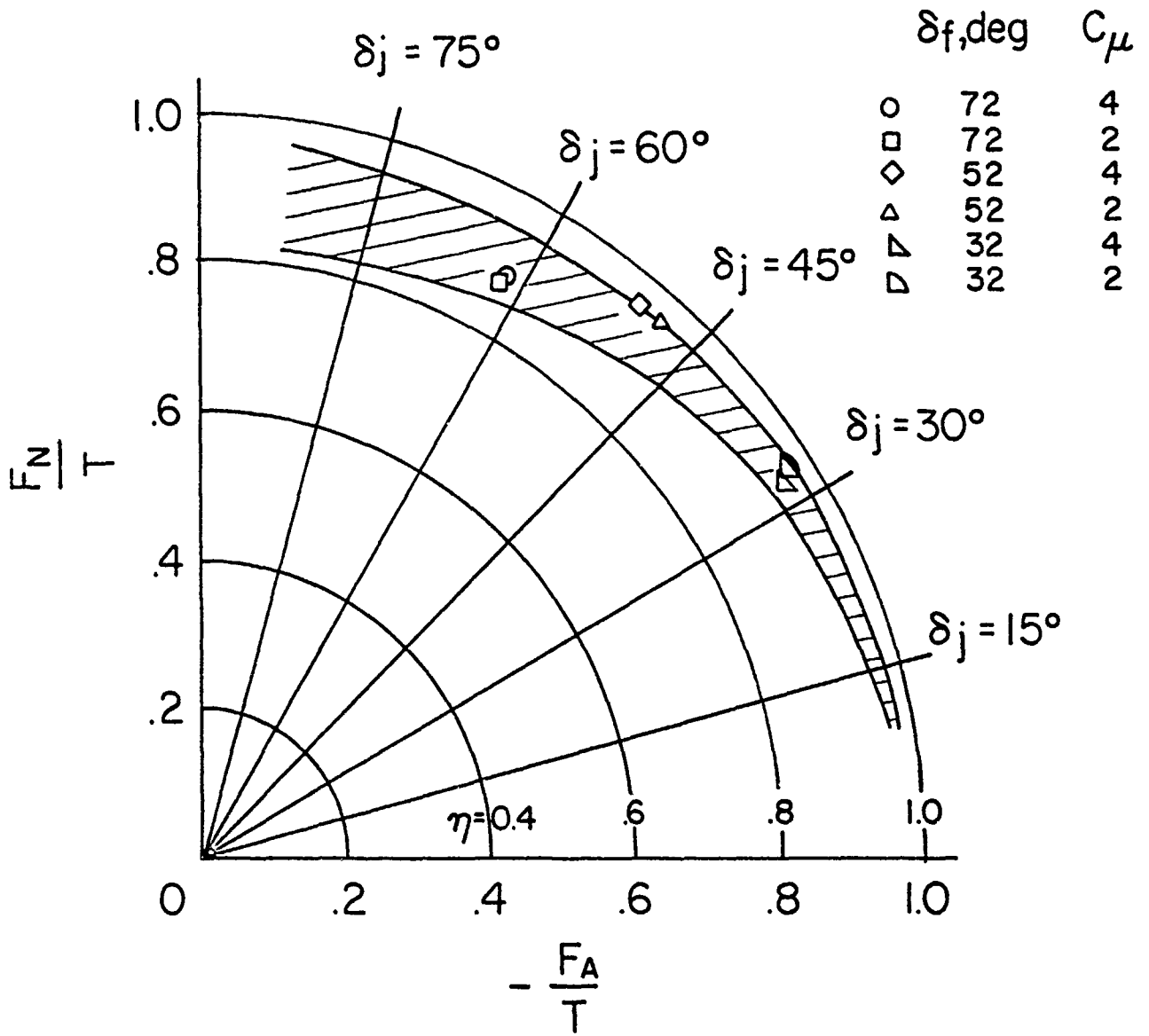


Figure 2 Summary of Static Turning Characteristics

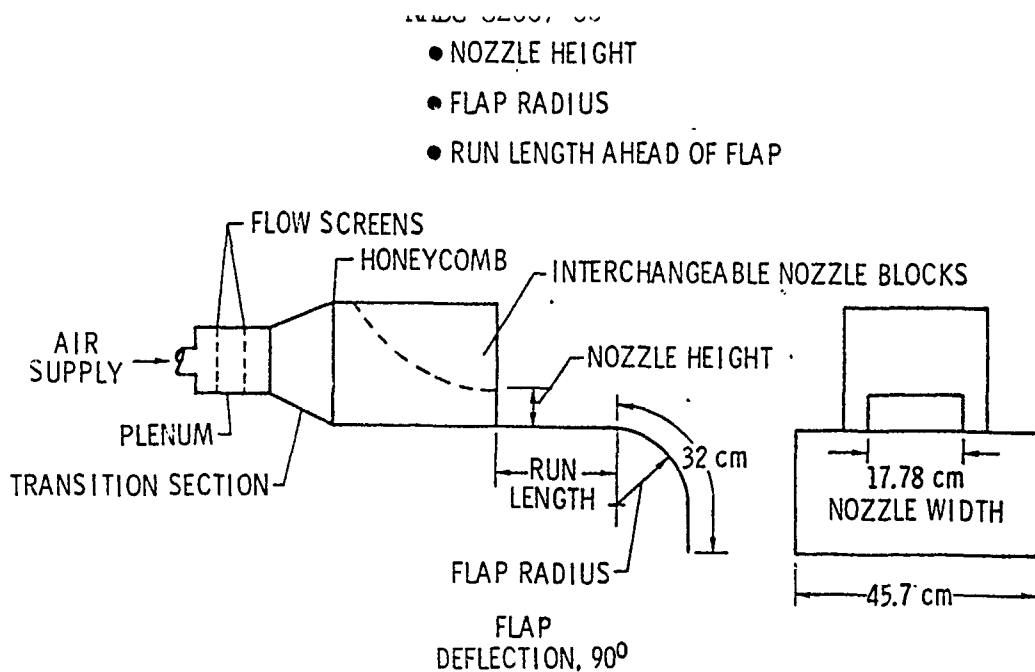


Figure 3 Model Configuration Used in Static Test of USB Nozzle and Flap Variables (Reference 3)

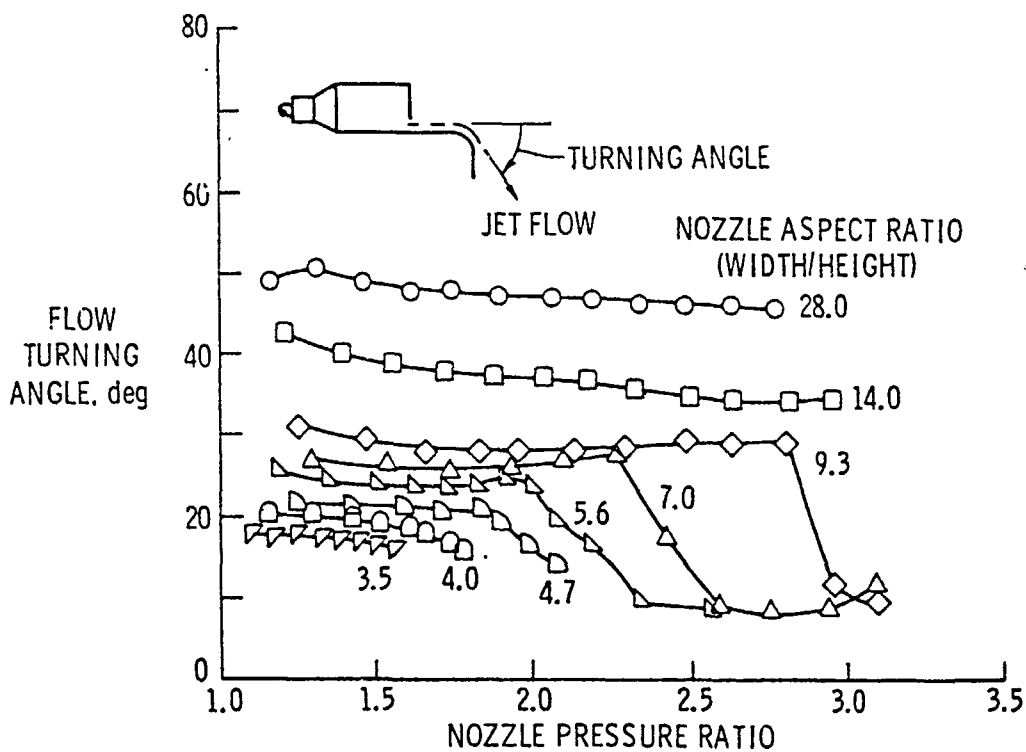


Figure 4 Effect of Pressure Ratio on Flow Turning for Various Nozzle Aspect Ratios

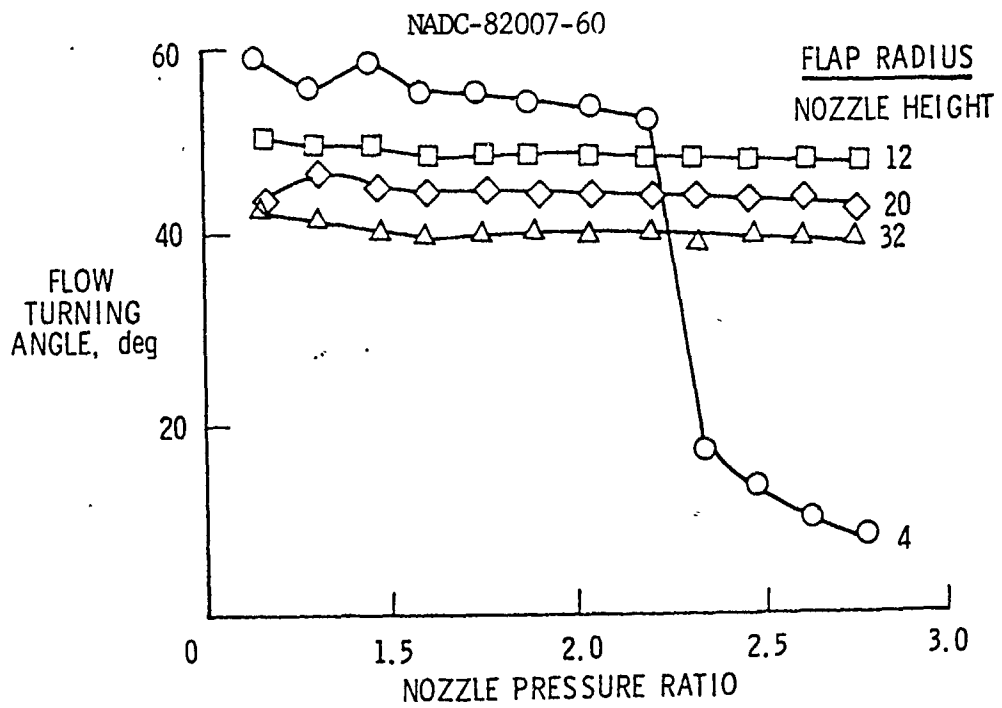


Figure 5 Effect of Pressure Ratio on Flow Turning for a Range of Flap Radius. Nozzle Aspect Ratio of 28

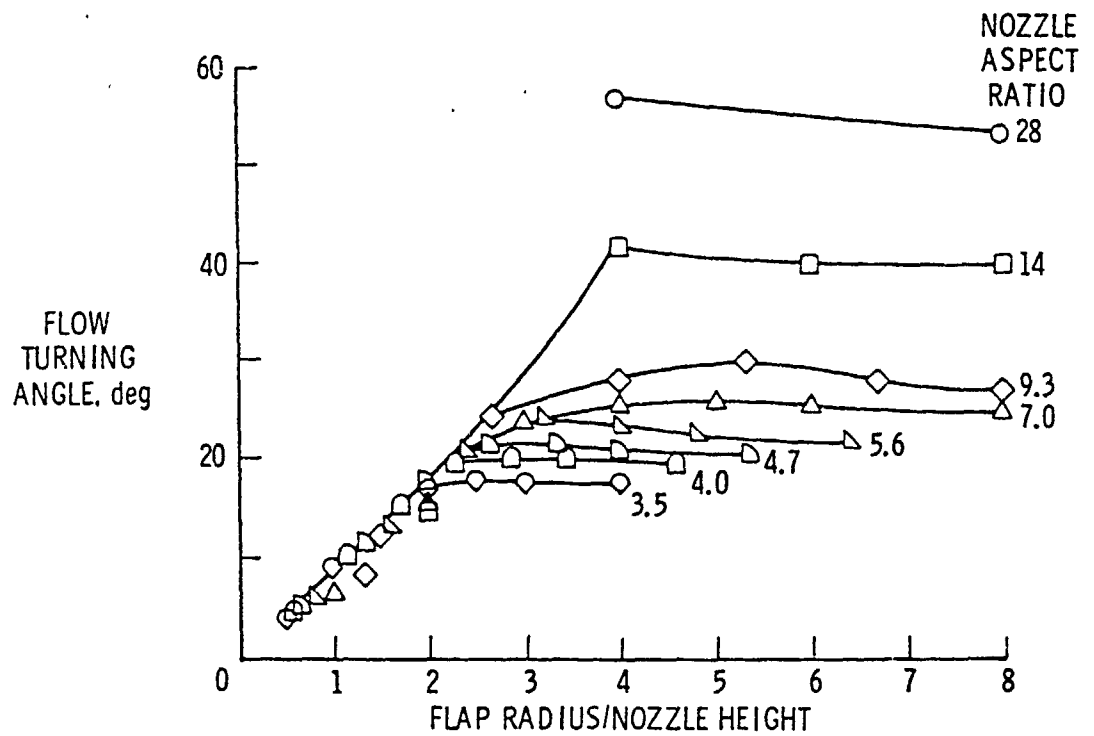


Figure 6 Effect of Flap Radius of Flow Turning for A Pressure Ratio of 1.4 and a Constant Run Length

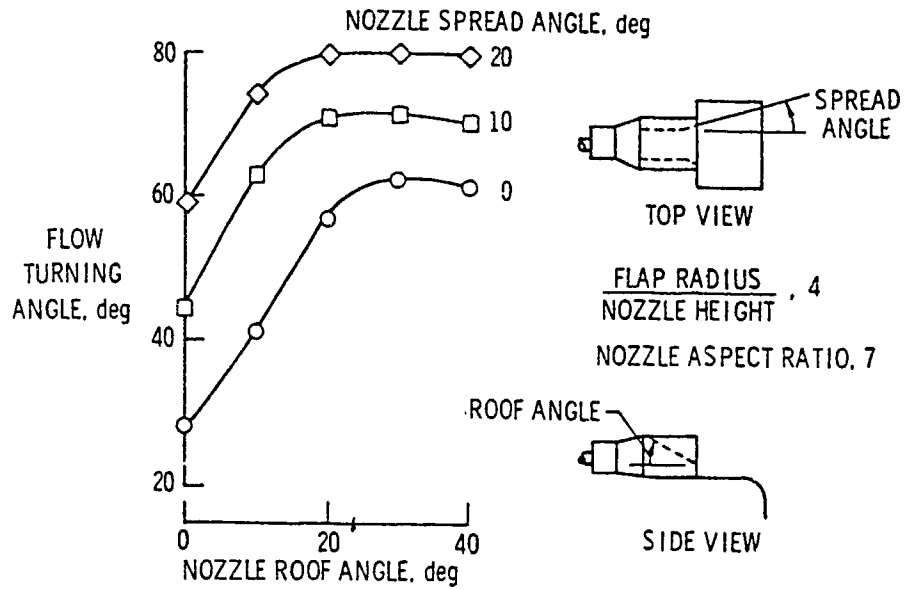


Figure 7 Effects of Nozzle Roof Angle and Spread Angle on Flow Turning

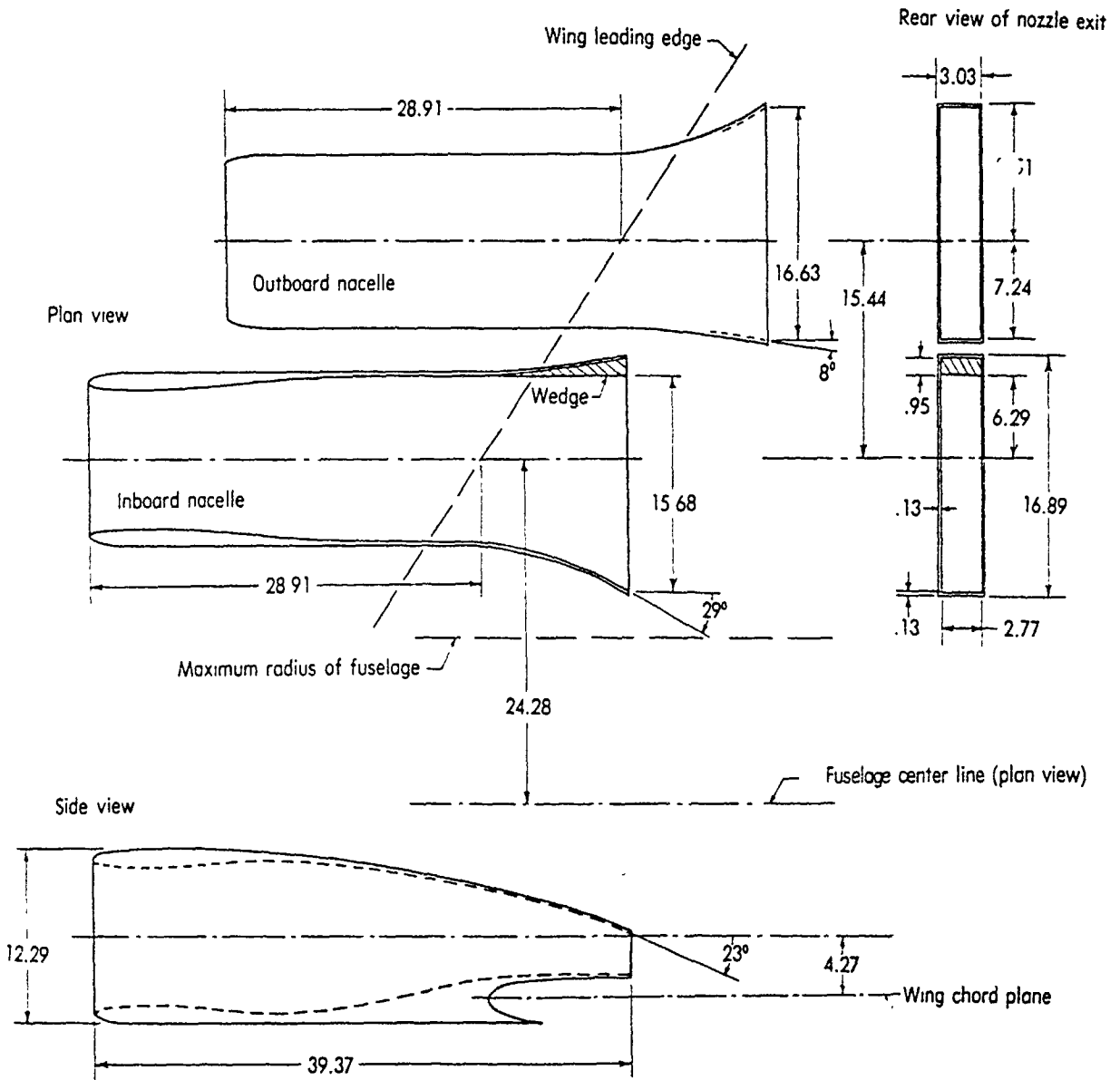


Figure 8 Details of Nacelles and Aspect-Ratio-6 Rectangular Nozzles

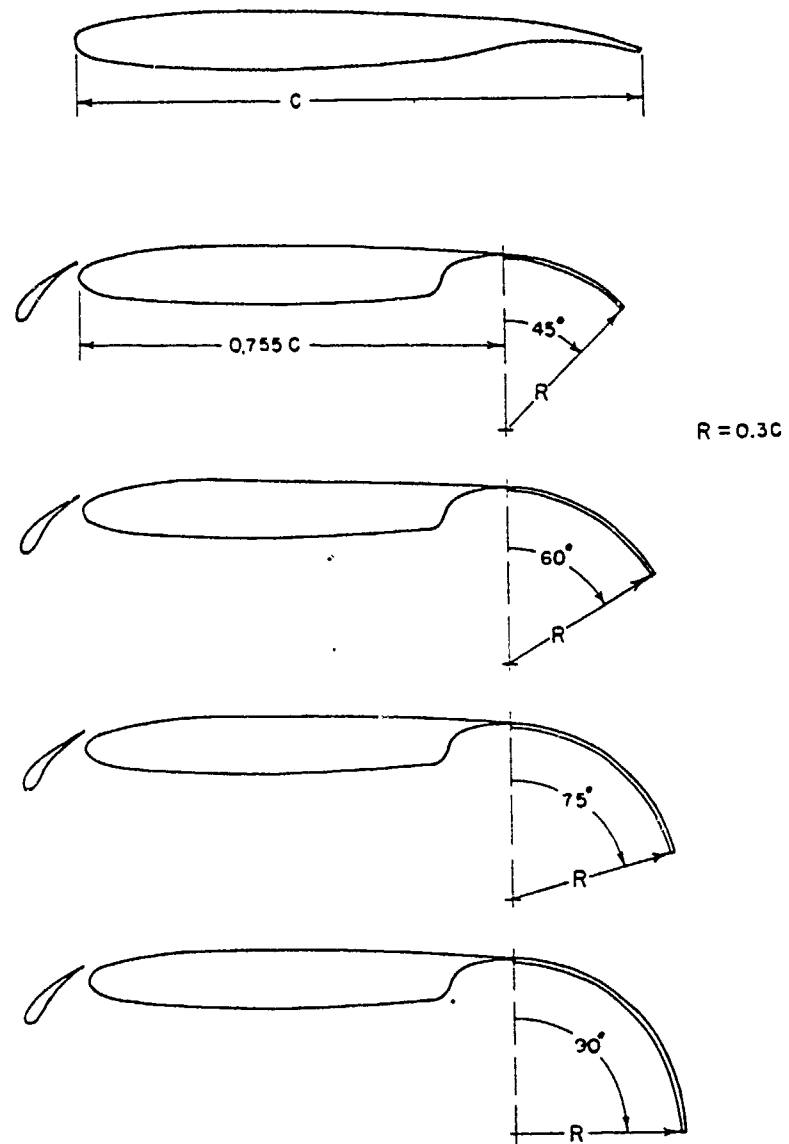


Figure 9 Radius Flap High-Lift System

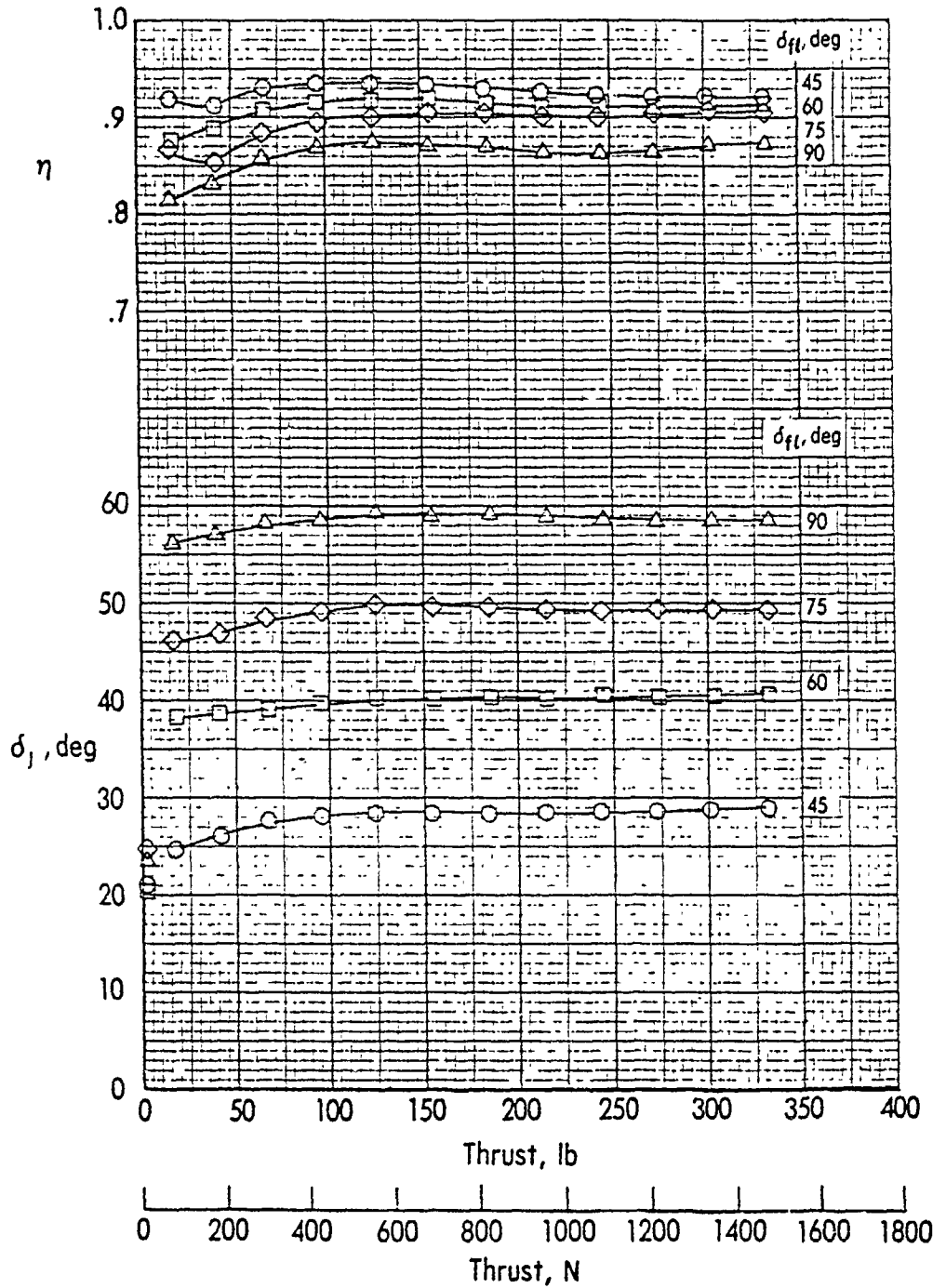


Figure 10 Variation of Static Turning Angle and Turning Efficiency with Static Thrust. Rectangular Nozzles and Radius Flap

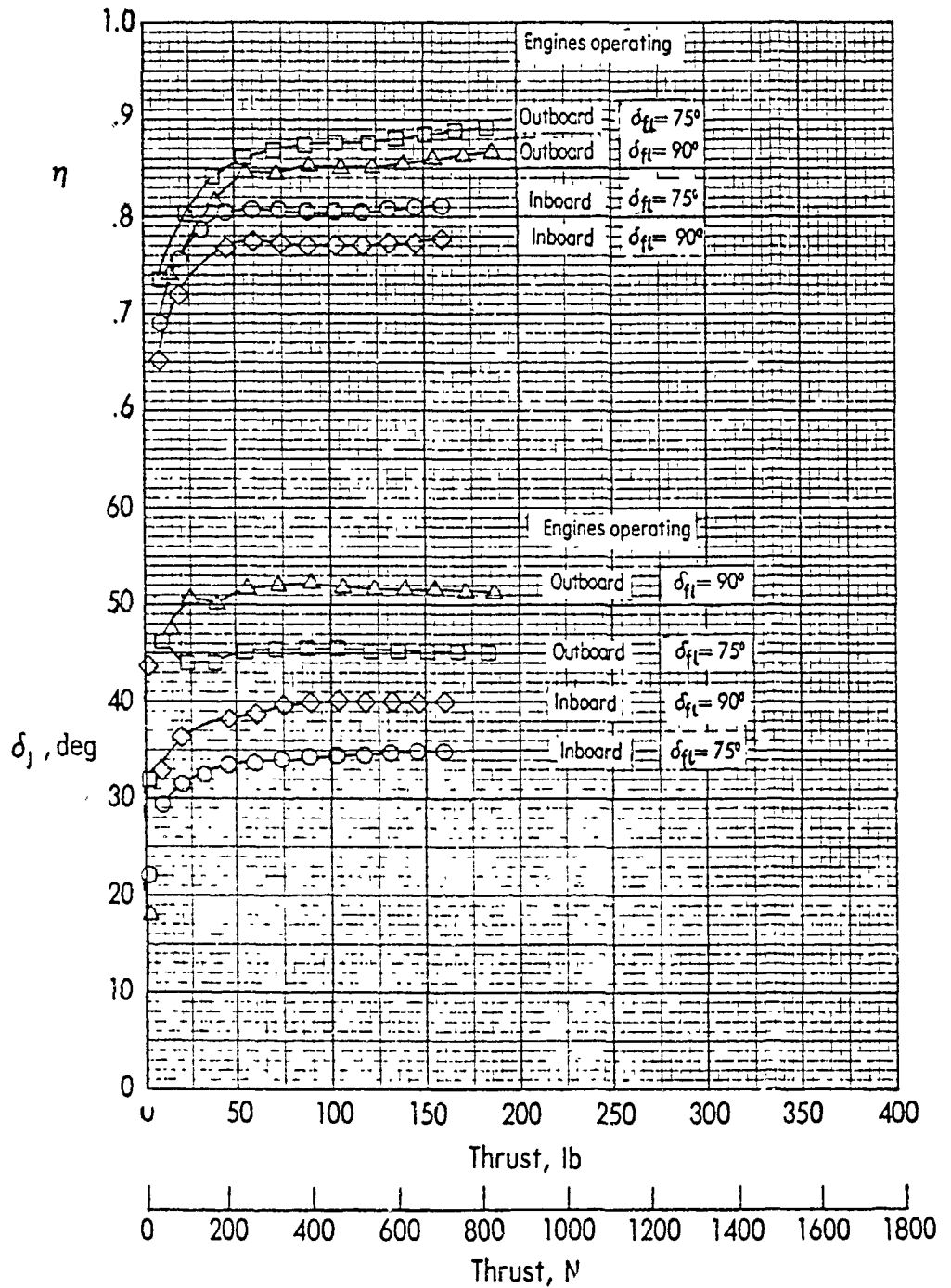


Figure 11 Variation of Static Turning Angle and Turning Efficiency with Twin-Engine Simulation. Rectangular Nozzles and Radius Flap

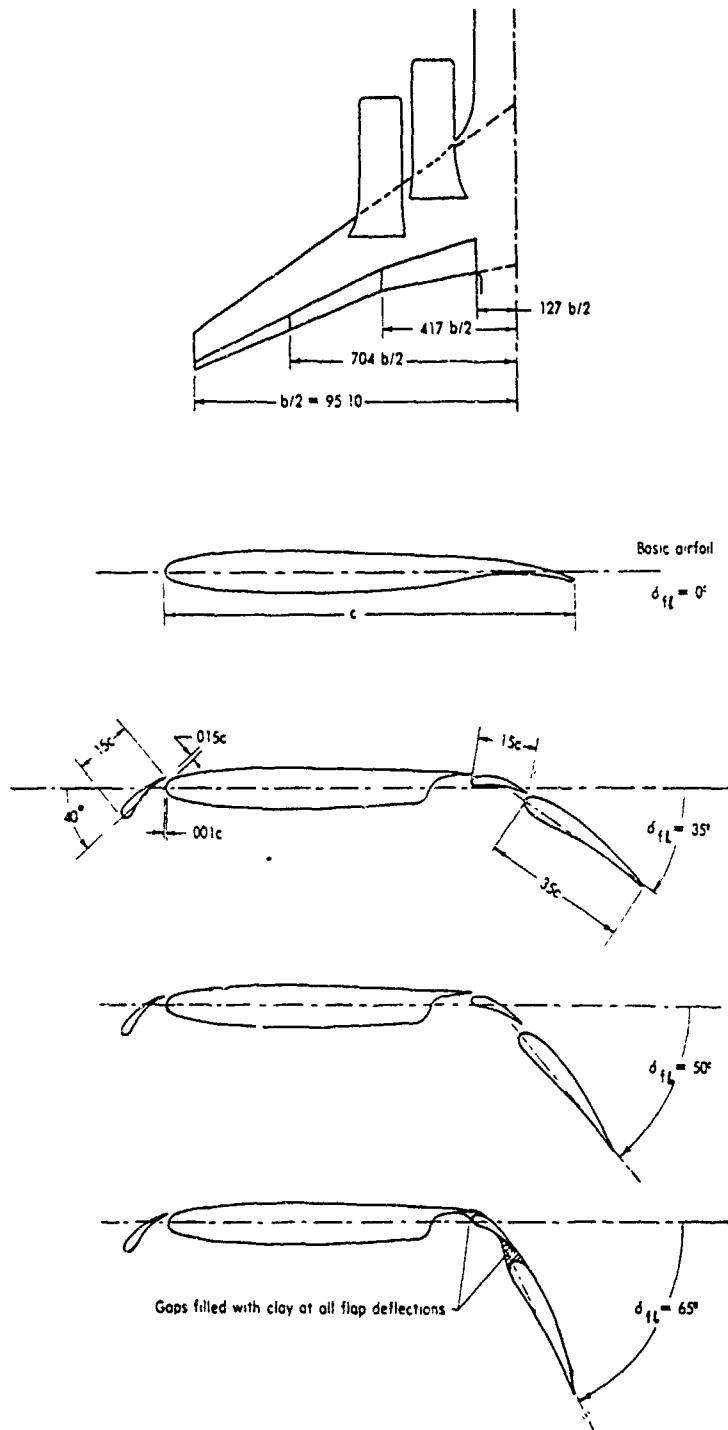


Figure 12 Basic High Lift System with Double-Slotted Flap

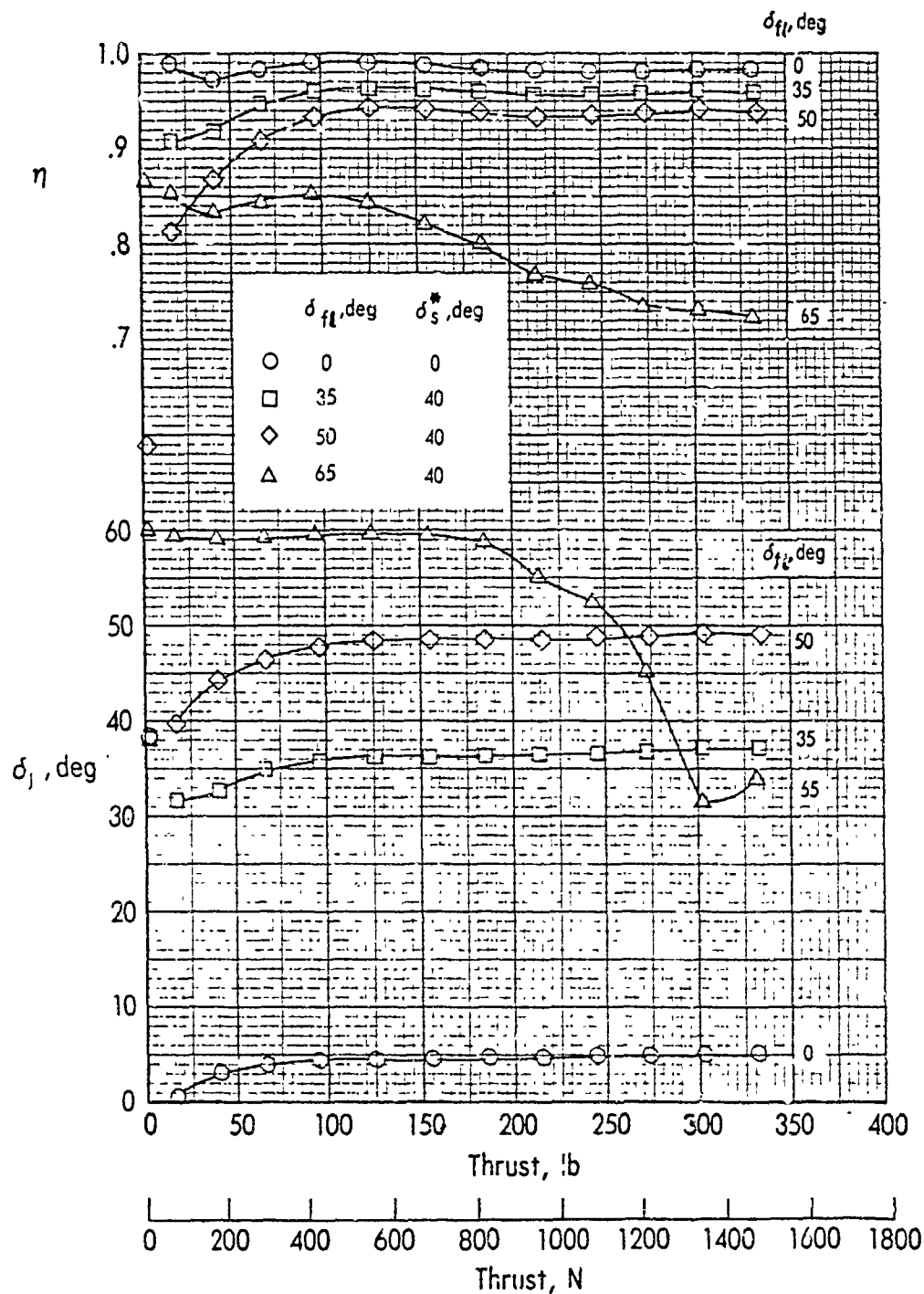


Figure 13 Variation of Static Turning Angle and Turning Efficiency. Rectangular Nozzles and Basic Flap

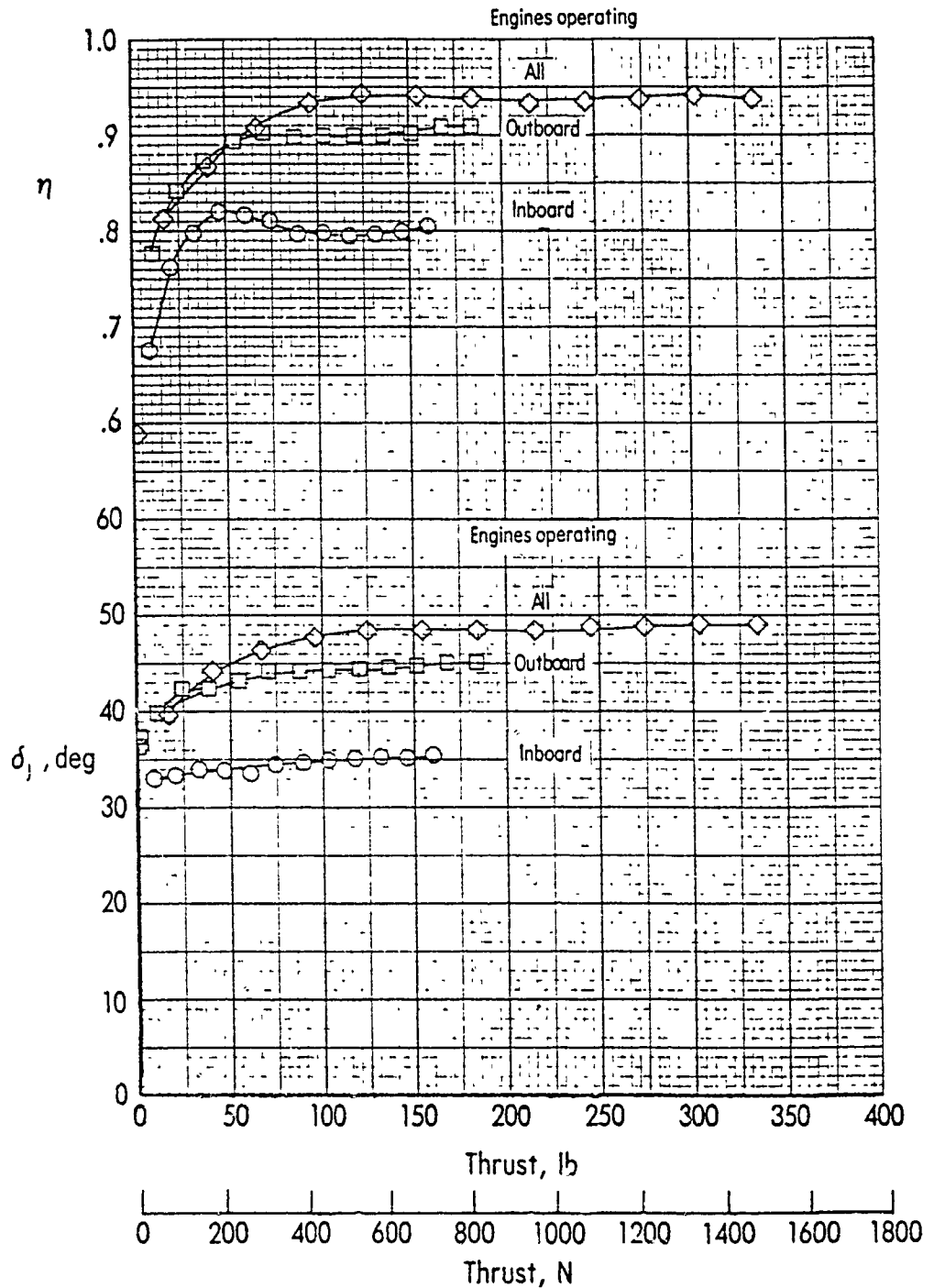


Figure 14 Variation of Static Turning Angle and Turning Efficiency with Twin-Engine Simulation. Rectangular Nozzles and Basic Flap

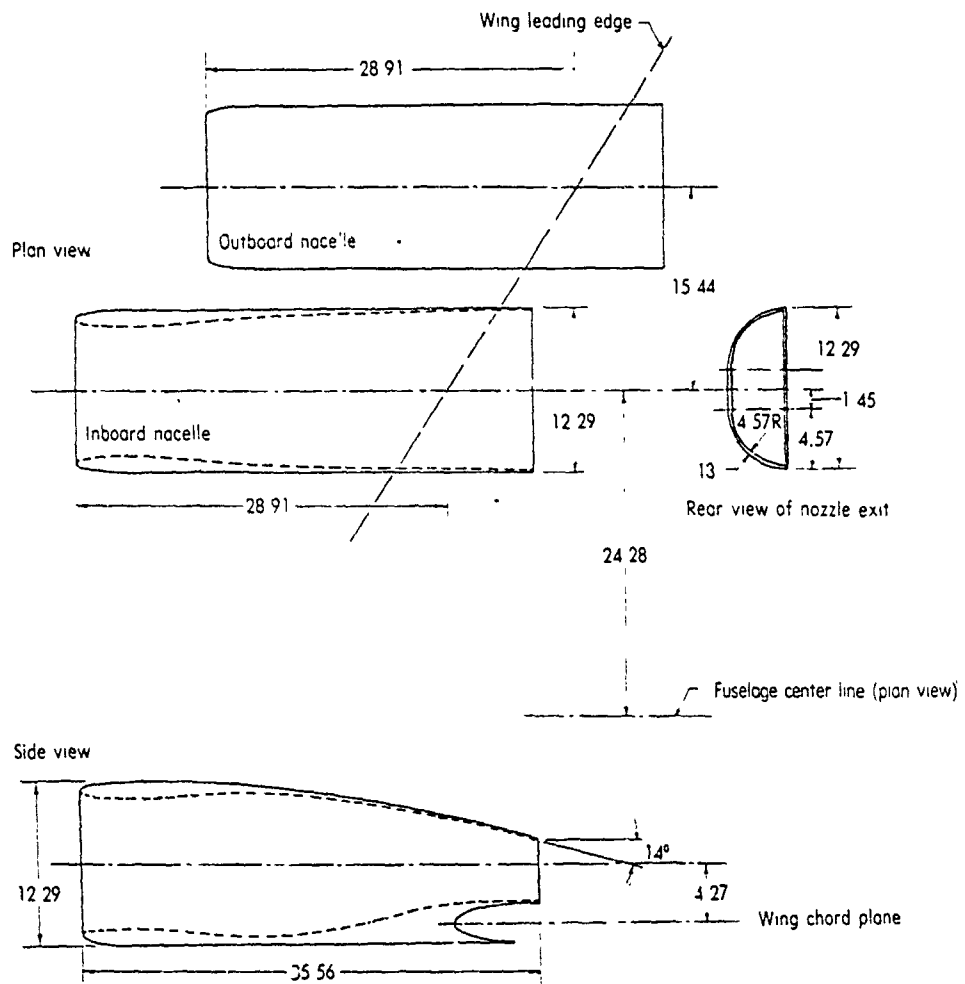


Figure 15 Details of Nacelles and D-Nozzles

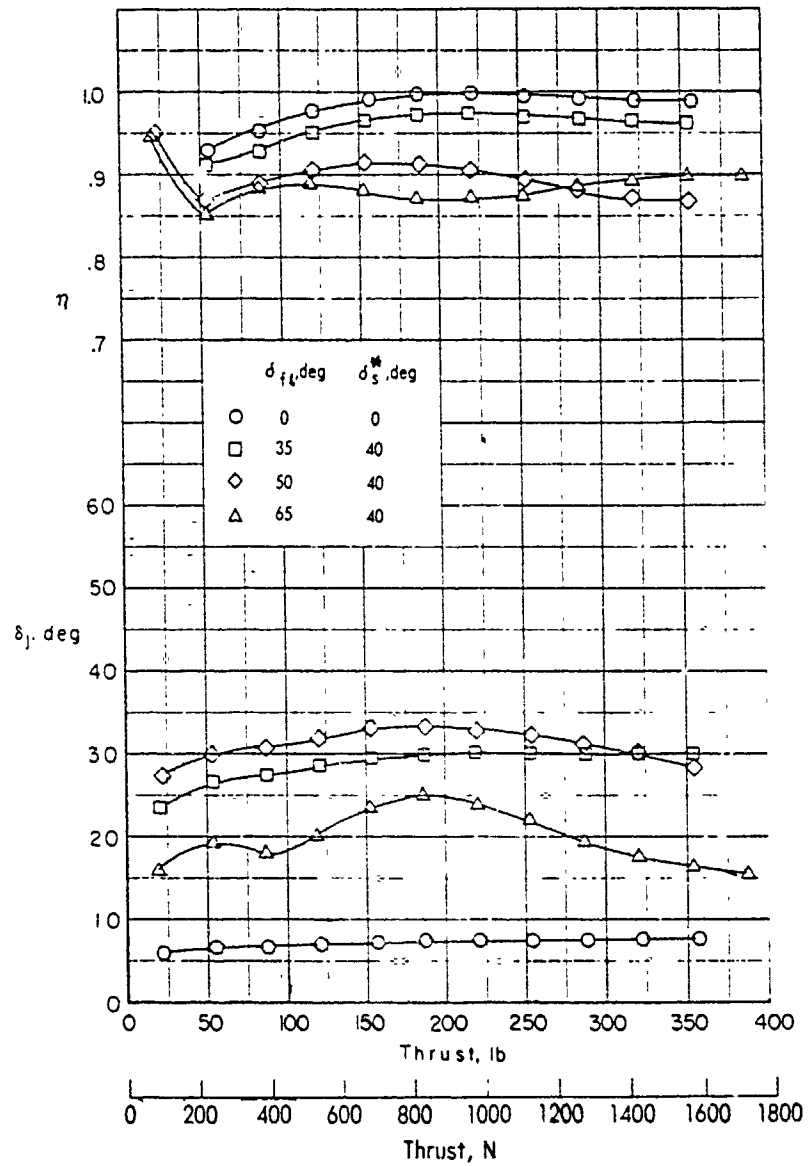


Figure 16 Variation of Static Turning Angle and Turning Efficiency with Static Thrust. D-Nozzles and Basic Flap

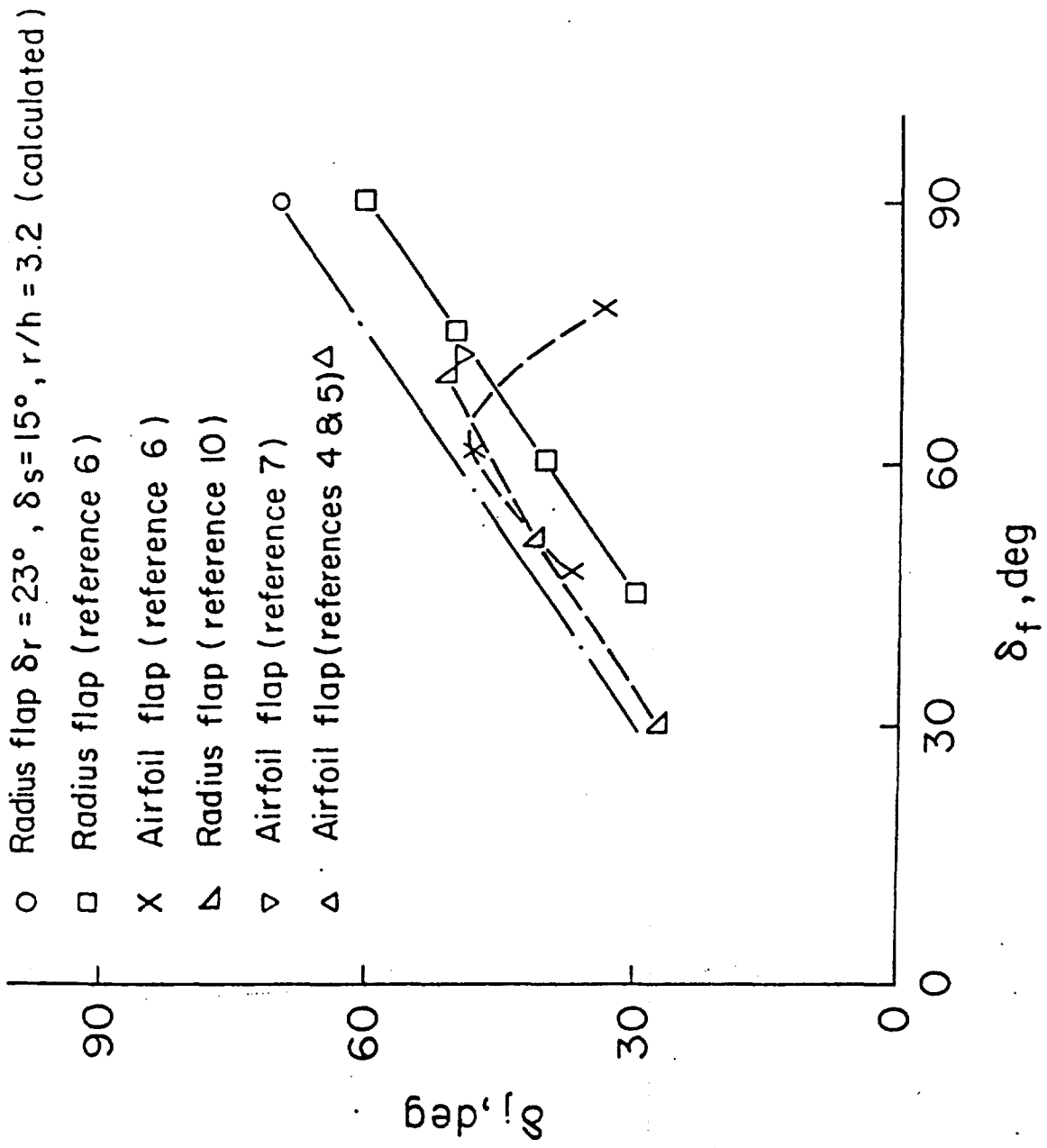


Figure 17 Static Turning Angle for Rectangular Nozzles with Aspect Ratio Equal to 6 and Various Flap Systems

- ▽ Radius flap (calculated)
- Radius flap (reference 6)
- X Airfoil flap (reference 4)
- △ Airfoil flap (reference 5)
- ▷ Airfoil flap (reference 7)
- D nozzle, VG retracted (reference 8)
- ∅ D nozzle, with VG (reference 8)

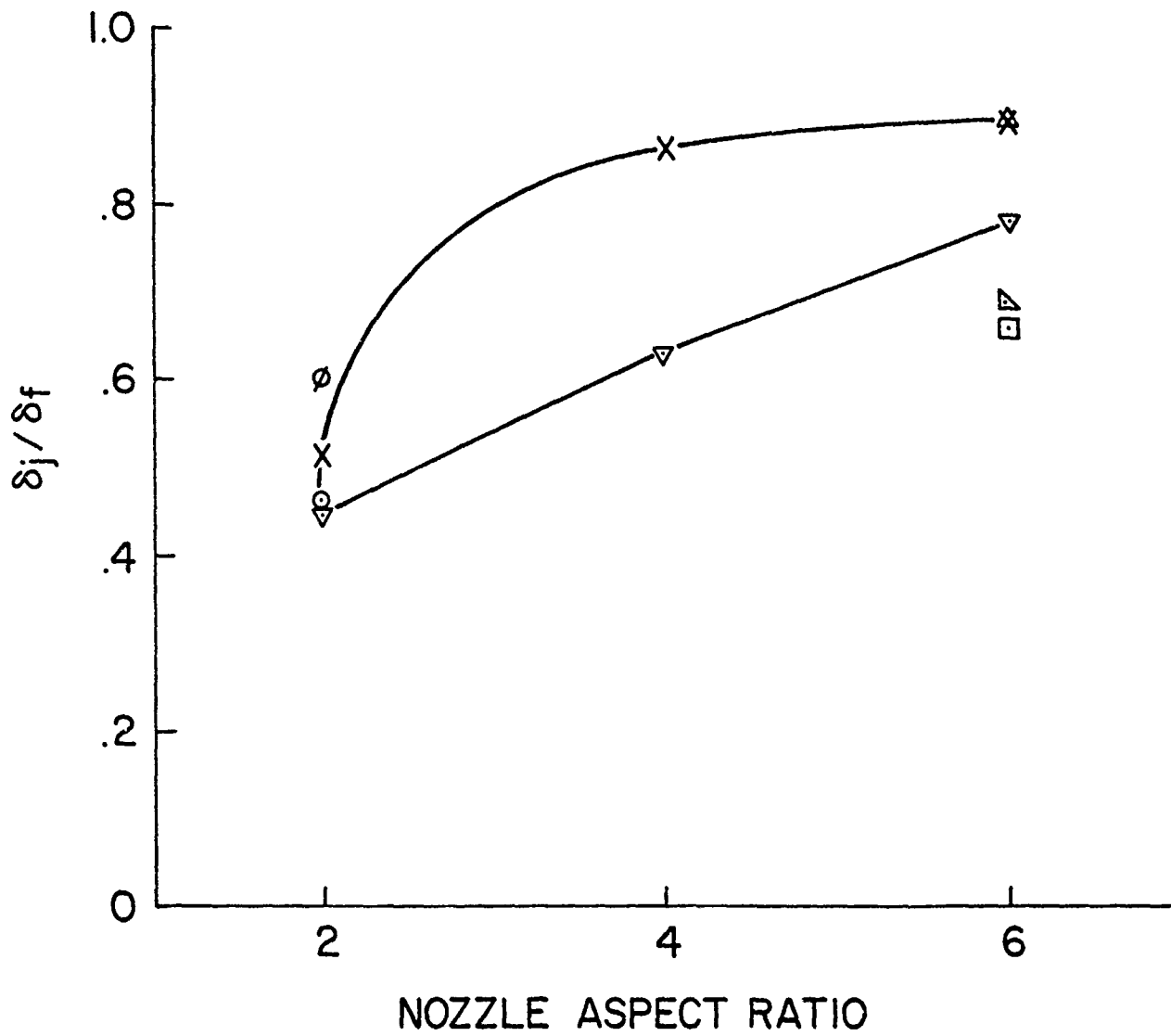


Figure 18 Static Turning Angle for Rectangular Nozzles and Various Flap Systems

TABLE 1 EXPERIMENTAL DATA

Nozzle		Flap	Aircraft Model	Data Source	Reference
Shape	Geometry				
Rectangular	Various	Radius	Not installed	NASA SP 406	3
Rectangular	AR 6	Radius	Not installed	NASA TND-7816	10
Rectangular	AR 6	Radius	Four-engine model Wing AR 7.48	NASA TND-8061	6
Rectangular	AR 6	Airfoil	Four-engine model Wing AR 7.48	NASA TND-8061	6
Rectangular	AR 2,4,6	Airfoil	Semi-span one-engine model, Wing AR 7.8	NASA TND-7526	4
Rectangular	AR 2,4,6	Airfoil	Semi-span one-engine model, Wing AR ?	SAE 740470	5
Rectangular	AR 4.5	Airfoil	Four-engine model Wing AR 7	NASA TND-7399	11
Rectangular	AR 6	Airfoil	Two-engine model Wing AR 5.76	NASA TND-8235	7
D	AR = 2	Airfoil	Not installed	NASA SP 406	8
D	AR 2.63	Airfoil	Four-engine model Wing AR 7.48	NASA TND-8061	6
Deflectors		Airfoil	Semi-span two-engine model, Wing AR 3.92	NASA TND-7183	10

D I S T R I B U T I O N L I S T

REPORT NO. NADC-82007 -60

AIRTASK NO. A03V-320D/01B/7F41-400-000

No. of Copi

NAVAIRSYSCOM.	4
(2 for AIR-950D)	
(1 for AIR-320D)	
(1 for AIR-5301)	
NAVWPNCEN, China Lake, CA	1
NAVAIRPROPCEN, Trenton, NJ.	1
DTNSRDC, Bethesda, MD (Attn: Dr. H. Chaplin)	1
ONR, Arlington, VA (Attn: R. Whitehead)	1
NAVPGSCOL, Monterey, CA (Attn: M. Platzer)	1
NASA, Ames Research Center, Moffett Field, CA	2
(1 for D. Hickey)	
(1 for W. Deckert)	
NASA, Langley Research Center, Hampton, VA (Attn: R. Margason)	1
NASA, Lewis Research Center, Cleveland, OH.	1
Wright-Patterson AFB, Dayton, OH.	2
(1 for Flight Dynamics Lab)	
(1 for Aeronautical Systems Division)	
The Pentagon, Washington, DC (Attn: R. Siewert)	1
U.S. Army Aviation Systems Command, St. Louis, MO	1
U.S. Army Research Office, Durham, NC	1
DTIC, Alexandria, VA.	12
Boeing Company, Seattle, WA (Attn: E. Omar).	1
LTV-Aerospace Corporation, Dallas, TX	2
(1 for T. Beatty)	
(1 for W. Simpkin)	
Rockwell International, Columbus, OH (Attn: W. Palmer)	1
General Dynamics Corporation, Ft. Worth, TX (Attn: W. Folley).	1
Nielson Engineering, Mountain View, CA (Attn: S. Spangler)	1
Univ. of Tennessee, Space Inst., Tullahoma, TN (Attn: W. Jacobs)	1
Lockheed-California Co., Burgank, CA (Attn: Y. Chin)	1
Northrop Corporation, Hawthorne, CA (Attn: P. Wooler).	1
Grumman Aerospace Corp., Bethpage, LI, NY (Attn: D. Migdal).	1
Royal Aeronautical Establishment, Bedford, England (Attn: A. Woodfield).	1
Fairchild-Republic, Corporation, Farmingdale, LI, NY.	1
Calspan, Buffalo, NY.	1
McDonnell Douglas Corp., St. Louis, MO (Attn: Dr. D. Kotansky)	1
V/STOL Consultant, Newport News, VA (Attn: R. Kuhn).	1
Georgia Inst., of Technology, Atlanta, GA (Attn: Dr. H. McMahon)	1
Penn State Univ., Univ. Park, PA (Attn: Prof. B. W. McCormick)	1